

Improvements to the hydrological processes of the Town Energy Balance Model (TEB-Veg, SURFEX v7.3) for urban modelling and impact assessment

Xenia Stavropulos-Laffaille¹, Katia Chancibault¹, Jean-Marc Brun¹, Aude Lemonsu², Valery Masson²,
5 Aaron Boone², Hervé Andrieu¹

¹IFSTTAR, GERS, EE, F-44344 Bouguenais, France

²CNRM UMR 3589, Météo-France/CNRS, Toulouse, 31057 Toulouse CEDEX 1, France

Correspondence to: Xenia Stavropulos-Laffaille (xenia.laffaille@ifsttar.fr)

Abstract. Climate change and demographic pressures are affecting both the urban water balance and microclimate, thus
10 amplifying the urban flooding and urban heat island phenomena. These issues need to be addressed when engaging in urban
planning activities. Local authorities and stakeholders have therefore opted for more nature-based adaptation strategies, which
are especially suitable in influencing both hydrological and energy processes. Assessing the multiple benefits of such strategies
on the urban microclimate requires effective numerical tools. This paper presents recent developments focusing on the water
budget in the TEB-Veg model (SURFEX v7.3), which allows for a more complete representation of the hydrological processes
15 taking place in urban subsoil. This new hydrological module is called TEB-Hydro. The inherent developments feature: the
introduction of subsoil beneath built surfaces, the horizontal rebalancing of intra-mesh soil moisture, soil water drainage via
the sewer network, and the limitation of deep drainage. A sensitivity analysis is then performed in order to identify the
hydrological parameters required for model calibration. The new TEB-Hydro model is evaluated on two small residential
catchments in Nantes (France), over two different periods, by comparing simulated sewer discharges with observed findings.
20 In both cases, the model tends to overestimate total sewer discharge and performs better under wet climate conditions, with a
KGE statistical criterion greater than 0.80 vs. approximately 0.60 under drier weather conditions. These findings are definitely
encouraging since the same set of model parameters are identified for both catchments, irrespective of meteorological and
local physical conditions. This approach offers opportunities to apply the TEB-Hydro model at the city scale in regard to
projections of climate and demographic changes.

25 1. Introduction

Cities consume space and energy, generate pollution and nuisances, and are vulnerable to natural or manmade hazards, such
as floods and urban heat islands (hereafter denoted UHI), and climate change is likely to exacerbate all these phenomena (EEA,
2012).

Adapting cities to global changes (climate change and demographic pressures) has become a major challenge in the field of planning policy. The use of nature-based solutions (hereafter denoted NBSs), such as green and blue infrastructure, has been approved as part of sustainable urban development (Sustainable Urban Drainage Systems, water and pollution source control, insulation of buildings) and is therefore recommended (Hamel *et al.*, 2013; EC, 2015). Evaluating such adaptation and mitigation strategies however requires conducting impact studies capable of assessing the various services these solutions can offer, along with their corresponding interactions (energy, thermal comfort, water, landscaping, etc.) (Bach *et al.*, 2014). With regards to hydro-microclimatic patterns, the integration of urban green spaces and vegetation allows increasing water infiltration as well as evapotranspiration (or latent heat flux). For modelling purposes, evapotranspiration is thus a key element since it affects both the urban water and energy budgets (Mitchell *et al.*, 2008).

Despite the increased interest in urban hydrology over recent years (Fletcher *et al.*, 2013; Hamel *et al.*, 2013; Shirmer *et al.*, 2013; Salvadore *et al.*, 2015), the various water- and energy-related processes are still rarely addressed with the same level of detail, and the coupling between them is often oversimplified.

In the past, the emphasis on the urban water cycle was directed at designing of urban drainage systems and their operations under extreme events (flooding). Hydraulic models have thus been used to analyse rainfall-runoff patterns during rain events when evapotranspiration is not a major concern (Berthier *et al.*, 2006; Fletcher *et al.*, 2013). In recent decades however, a more decentralised urban water management system has necessitated impact studies that focus on the urban water cycle as a whole. Consequently, urban hydrological models are being more heavily promoted, as opposed to hydraulic models. Yet these hydrological models still use a simple energy balance. Evapotranspiration is often calculated from a reference value of potential evapotranspiration, which takes into account soil moisture conditions and in some instances vegetation (DHI, 2001; Rodriguez *et al.*, 2008; Rossman, 2010). At the local level, atmospheric demand is typically not considered as a limiting factor for evapotranspiration, and a direct interaction rarely exists between water balance and energy balance. In their state-of-the-art paper, Fletcher *et al.* (2013) noted that evapotranspiration in urban areas remains relatively poorly explored.

Unlike hydrological models, the urban micro-climate models (Masson, 2000; Musy *et al.*, 2015; Gros *et al.*, 2016) provide a detailed solution of energy and radiative budgets. However, the water balance is often simplified in micro-climate models, which can lead to an alteration of the modelled latent heat fluxes (Grimmond *et al.*, 2011). Malys *et al.* (2016) used such a model with “SOLENE-microclimat” to evaluate the mitigation effects of vegetation on UHI. In this model however, soil moisture is not considered as a limiting factor, potentially leading to an overestimation of the cooling abilities of plants, especially under hot climate conditions. For example, the Town Energy Balance Scheme (TEB) described by Masson (2000) is a mesoscale surface scheme dedicated to the urban environment. The urban environment is presented in a simplified manner by means of the street canyon approach (Oke, 1987). This approach averages the characteristics of urban covers and morphology (building height, construction materials, canyon aspect ratio, street orientation) inside a single grid mesh. This approach initially resolves detailed energy and radiative budgets of built-up areas (buildings and roads). However, the hydrological part is presented more simply, i.e.: i) artificial surfaces (buildings and roads) are completely impervious and ii) water exchanges are thus only taken into account between the surface and the atmosphere. Lemonsu *et al.* (2007) then

introduced the rainfall interception capacities of built-up surfaces and integrated water infiltration through artificial surfaces, like roads, pavements and parking lots, into TEB in order to implement more realistic hydrological processes. The TEB model has evolved into TEB-Veg, by integrating vegetated surfaces inside the street canyon. This step was allowed by using the ISBA-DF model (Interaction Soil-Biosphere-Atmosphere - explicit vertical diffusion) (Boone *et al.*, 2000) as part of the urban fabric (Lemonsu *et al.*, 2012a). Interactions within the radiative, energy and water balances between natural and artificial surfaces are now considered. Nevertheless, even if a detailed water balance for the subsoil of natural surfaces is calculated, the water processes occurring in the subsoil of artificial surfaces and their interactions with the surface are still being neglected. The objective of this study is to develop a complete urban hydro-microclimate model, hereafter called TEB-Hydro, by integrating the subsoil under built-up surfaces and hydrological soil-surface interactions into the existing TEB-Veg model. This step will allow treating the energy and water budgets at the same level of detail, which is critical to the impact assessment of NBSs at a city scale. First, the model concept will be described. Since the energy and radiation components of the model have not changed, as fully described in Masson (2000) and Lemonsu *et al.* (2012a), focus will be placed on the model's hydrological component and recent model developments. Next, the experimental sites and observation data will be presented. The model evaluation will then be laid out in Section 4 by means of analysing the simulations performed by the new model version.

2. Description of the TEB-Hydro hydrological model

TEB-Hydro is an evolution of TEB-Veg, with SURFEX v7.3 (Lemonsu *et al.*, 2012a), and was developed on the SURFEX modelling platform (Masson *et al.*, 2013). It can be applied at the city scale as well as the catchment scale. Like TEB-Veg, TEB-Hydro is based on a regular grid mesh with a resolution varying between several hundred and several deca-meters. This model can be run either coupled with other meteorological models or in offline mode forced by observed atmospheric data. It combines two surface schemes: TEB (Masson, 2000) and ISBA-DF (Boone *et al.*, 2000), both of which run on an integrated tiling approach and describe energy and water exchanges between the urban and natural subsoils, the surface and atmosphere, respectively. The urban environment is represented by three compartments, namely buildings (roofs and walls), roads (streets, pavements and parking lots), and gardens. This section will present the new model developments based on the existing TEB-Veg model version. A general description of the hydrological processes will be laid out first, followed by a discussion of the new developments dedicated to hydrological processes in the urban subsoil (Fig. 1).

2.1 General principles of hydrological processes

Interactions between the energy balance (Eq. 1) and water balance (Eq. 2) are established via an explicit resolution of the evapotranspiration term (Eq. 3):

$$Q^* + Q_F = Q_H + Q_E + \Delta Q_S + \Delta Q_A \quad [W \ m^{-2}] \quad (1)$$

$$P + I = E + R + D + \Delta W \quad [kg \ m^{-2} \ s^{-1}] \quad (2)$$

$$Q_E = \frac{E}{L_v} \quad [W \ m^{-2}] \quad (3)$$

where Q^* is the net all-wave radiation, Q_F the anthropogenic heat flux, Q_H the sensible heat flux, Q_E the latent heat flux, ΔQ_S the heat flux storage, ΔQ_A the net advection heat flux, P the total precipitation, I the water generated from anthropogenic activities (irrigation), E the evapotranspiration, R the total runoff, D the deep drainage, ΔW the variation in water storage both on the surface and in the ground during the simulation period, and lastly L_v the latent heat of vaporisation ($J \ kg^{-1}$).

2.1.1 Evapotranspiration

Evaporation is calculated for each surface type E_* ($kg \ m^{-2} \ s^{-1}$) (Fig. 1). For built-up surfaces, this value depends on both the surface specific humidity at saturation and the air humidity (inside the canyon for roads and above the canopy level for roofs) (Masson, 2000). Limitations are set by the maximum surface retention capacity of roofs $W_{max,rf}^{surf}$ (mm) and roads $W_{max,rd}^{surf}$ (mm), as represented by the surface water reservoirs. For natural surfaces, the various contributions from vegetation and natural subsoil are considered (Eq. 4) (Lemonsu *et al.*, 2012a):

$$E_{gdn} = E_{veg} + E_{gr} + E_{gr,i} + E_s \quad (4)$$

where E_{veg} is the vegetation evapotranspiration, $E_{gr,i}$ and E_{gr} the evaporation from bare soil respectively with and without freezing, and E_s the sublimation from snow. These terms are detailed in the SURFEX scientific documentation (https://www.umr-cnrm.fr/surfex/IMG/pdf/surfex_scidoc_v2-2.pdf).

2.1.2 Water interception

The water content changes in the interception water reservoirs of each surface type (denoted W_*^{surf} in mm) are affected by precipitation and evapotranspiration rates, as indicated in Masson (2000) and Lemonsu *et al.* (2012a):

$$\frac{\partial W_*^{surf}}{\partial t} = P - \frac{E_*}{L_v} \quad (5)$$

where * stands for rooftops, vegetation or bare ground surfaces.

For the road interception reservoir, the original evolution equation has been modified by including a slight water infiltration rate (I_{rd}) ($m \ s^{-1}$), since roads are never totally impervious (Ramier *et al.*, 2011):

$$\frac{\partial W_{rd}^{surf}}{\partial t} = P - \frac{E_{rd}}{L_v} - I_{rd} \quad (6)$$

I_{rd} is defined as a constant value over which the model must be calibrated. Typical values for this parameter can be found in Ramier *et al.* (2011).

2.1.3 Surface runoff

According to Masson (2000), when W_*^{surf} (mm) exceeds the maximum reservoir capacity ($W_{max,*}^{surf}$), surface runoff is produced (R_*^{surf} in mm s^{-1}). Henceforth, it is collected by the stormwater sewer network, depending on the effective connected impervious area fraction (f_{con}) (Sutherland, 2000). Surface runoff not collected by the stormwater sewer network ($(R_{rf}^{surf} +$
5 $R_{rd}^{surf}) * (1 - f_{con})$) is then added to the throughfall over natural surfaces, where it can infiltrate into the subsoil with a maximum infiltration capacity, according to the Green-Ampt approach (Abramopoulos *et al.*, 1988; Entekhabi and Eagleson, 1989; Lemonsu *et al.*, 2012a).

The urban runoff R_{town} (mm s^{-1}), which is used to determine the total stormwater sewer discharge (Q_{town}^{tot}), is composed of several sources, namely:

$$10 \quad R_{town} = R_{rf}^{surf} * f_{con} + R_{rd}^{surf} * f_{con} + R_{sew} + R_*^{subsurf} \quad (7)$$

where $R_{rf}^{surf} * f_{con}$ and $R_{rd}^{surf} * f_{con}$ are respectively the roof and the road surface runoff connected to the sewer network (in mm s^{-1}); R_{sew} is the runoff in the sewer network due to soil water infiltration (mm s^{-1}), and $R_*^{subsurf}$ the subsurface runoff from each compartment (mm s^{-1}) calculated in Eq. 16.

2.1.4 Vertical water transfer

15 The surface water infiltration, as described above, constitutes an input to the subsoil of both the garden compartment and road compartment. The water is then transferred vertically from layer to layer, accounting for the liquid water transfer and water vapour transfer stated in Boone *et al.* (2000). This process depends solely on pressure gradients, which enables taking different hydraulic soil properties into consideration. At the bottom of each soil column, the vertical water transfer is adapted by taking boundary conditions into account. The resulting outgoing water flux of the model is called deep drainage D_* , and this parameter
20 has been slightly modified for TEB-Hydro (Sect. 2.2.3).

2.2 Inclusion of hydrological processes in the urban subsoil

In accordance with the soil description of urban gardens provided in Lemonsu *et al.* (2012a), soil compartments are now considered under within the category of built-up surfaces, namely roads and buildings (Fig. 1). All three soil columns are
25 represented by horizontal layers, with an identical vertical grid in order to compute subsurface soil water transport. The thickness of each layer increases downward, with a higher grid resolution on top. In the case of the road compartment, the upper soil layers are represented by structural layers in accordance with Bouilloud *et al.* (2009). By integrating natural soil below urban surfaces, the hydrological processes in the soil (vertical water transfer and deep drainage) of both road and building compartments are being adapted from the garden compartment. Water infiltration through the road structure is thus

now considered as a recharge of soil moisture in the road compartment soil column. No water however is input into the building compartment soil column.

2.2.1 Horizontal water transfer

The lateral water interactions of each soil layer, from among the three distinct compartments of the same grid cell, have been added (Fig. 1). In considering the structural layers of the road compartment, the horizontal transfer in the upper soil layers is computed solely between the garden and building compartments. Below that level, all three compartments are taken into account.

This approach is based on the principle of an exponential decay in the water content, tending towards the mean soil moisture of all three compartments, which is limited by soil moisture content at the wilting point. The soil texture is assumed to be homogeneous for all three compartments within a given grid cell. Moreover, no lateral transfer is taking place between the grid cells of the model. The lateral intra-mesh soil moisture transfer for each soil layer is described as follows:

$$\frac{\partial W_*^{gr}}{\partial t} = -\frac{1}{\tau} * \frac{\overline{K_{sat}}}{K_i} \quad (8)$$

Updating the soil moisture content in each layer and compartment after each time step yields:

$$W_*^{gr,'} = \overline{W^{gr}} + (W_*^{gr} - \overline{W^{gr}}) * \exp\left(-\left(\frac{1}{\tau} * \frac{\overline{K_{sat}}}{K_i}\right) * dt\right) \quad (9)$$

$$15 \text{ with: } \overline{W^{gr}} = \frac{\sum W_*^{gr} * f_*}{\sum f_*} \quad (10)$$

where W_*^{gr} and $W_*^{gr,'}$ are respectively the soil moisture content for each compartment before and after horizontal balancing ($\text{m}^3 \text{ m}^{-3}$), $\overline{W^{gr}}$ is the mean soil moisture content of all compartments before balancing ($\text{m}^3 \text{ m}^{-3}$), τ the time constant for one day, $\frac{\overline{K_{sat}}}{K_i}$ the ratio of the mean hydraulic conductivity at saturation of all three compartments to the hydraulic conductivity of each compartment, dt the numerical time step of the model (s), and f_* the fraction of each compartment.

20 2.2.2 Drainage of soil water via the sewer network

Various experiments and observations (Belhadj *et al.*, 1995; Lerner, 2002; Berthier *et al.*, 2004; Le Delliou *et al.*, 2009) have shown that soil water drainage occurs when artificial networks are exposed to saturated soil moisture conditions. The ISBA soil pattern however is intended to depict the unsaturated zone rather than the saturated zone. This pattern is based on a representation of the soil moisture state in agronomic terms (i.e. water content at wilting point, field capacity and saturation). When taking this representation into account, the infiltration rate into the sewer network (I_{sew} in m s^{-1}) is described in such a way that the hydraulic conductivity of the network soil layer ($k_{sew}(W_{gr})$ (m s^{-1})) serves as its limiting factor, with a maximum value at saturation:

$$I_{sew} = k_{sew}(W_{gr}) * I_p * D_{sew} \quad (11)$$

where I_p is a parameter without any physical significance, merely representing the sewer pipe water-tightness (-), which must be calibrated; and D_{sew} the sewer density within a single grid cell (-), as expressed by the ratio of the total sewer length in one grid cell (m) to the maximum total sewer length in a single grid cell of the entire study site (m). Let's note that this formulation has been adapted to TEB-Hydro from Rodriguez *et al.* (2008).

5 2.2.3 Deep drainage

In cities, artificial networks may play the role of rivers and thus contribute to draining soil water by means of infiltration. It has therefore been envisaged to limit deep drainage in order to favour soil water infiltration into the sewer networks during wet periods. For this purpose, the soil moisture emerging from the last layer of the model is partially or totally retained, according to a coefficient of recharge C_{rech} , until complete layer saturation. At each time step, the soil moisture content in the last layer n is thus updated according to:

$$W_*^{gr,n} = W_*^{gr,n} + W_*^{gr,flux,n} * C_{rech} \quad (12)$$

$$\text{And the deep drainage becomes: } D_* = W_*^{gr,flux,n} * (1 - C_{rech}) * d_n * \rho / dt \quad (13)$$

where $W_*^{gr,n}$ is the soil moisture content of the last layer n ($m^3 m^{-3}$), $W_*^{gr,flux,n}$ the soil moisture content derived from the outgoing water flux ($m^3 m^{-3}$), C_{rech} the coefficient of recharge (-) in order to limit deep drainage, D_* the deep drainage ($mm s^{-1}$), d_n the thickness of the last layer, ρ the water density ($kg m^{-3}$), and dt the numerical time step of the model (s).

If the deep layer is saturated, the excess moisture rises from layer to layer, with:

$$\text{The soil moisture content in upper layer } i-1: W_*^{gr,i-1,'} = W_*^{gr,i-1} + \max(0, W_*^{gr,i} - W_{*,sat}^{gr,i}) * \frac{d_{i-1}}{d_i} \quad (14)$$

$$\text{The soil moisture content remaining in layer } i: W_*^{gr,i,'} = \min(W_*^{gr,i}, W_{*,sat}^{gr,i}) \quad (15)$$

20 If saturation reaches the surface layer, then the excess moisture is added to subsurface runoff, i.e.:

$$R_*^{subsurf,'} = R_*^{subsurf} + \max(0, W_*^{gr,1} - W_{*,sat}^{gr,1}) * \frac{d_1}{dt} * \rho \quad (16)$$

where $W_{*,sat}^{gr,i}$ is the soil moisture content at saturation ($m^3 m^{-3}$), $W_*^{gr,i,'}$ and $W_*^{gr,i}$ respectively the soil moisture content in current layer i after and before update ($m^3 m^{-3}$), $W_*^{gr,i-1,'}$ and $W_*^{gr,i-1}$ respectively the soil moisture content in upper soil layer $i-1$ after and before update ($m^3 m^{-3}$), $\frac{d_{i-1}}{d_i}$ (-) the ratio of layer thicknesses between upper layer $i-1$ and lower layer i , and

25 $R_*^{subsurf,'}$ and $R_*^{subsurf}$ respectively the subsurface runoff after and before update ($mm s^{-1}$).

2.3 TEB-Hydro output variables

In addition to the simulated hydrological output variables calculated in TEB-Veg (latent heat fluxes on all surfaces, soil moisture in each soil layer ($W_{gdn}^{gr,i}$) and deep drainage (D_{gdn}) of the garden compartment), the TEB-Hydro model simulates soil moisture in each soil layer ($W_*^{gr,i}$) and the deep drainage (D_*) under artificial surfaces. Other new model output variables include urban runoff (R_{town}) in the stormwater sewer network, with its components stemming from rooftops ($R_{rf}^{surf} * f_{con}$) and road surfaces ($R_{rd}^{surf} * f_{con}$); soil water infiltration (R_{sew}); and the subsurface runoff from each compartment ($R_*^{subsurf}$).

3. Experimental study areas and observation data

The experimental data are derived from two small urban catchments in the city of Nantes (France). The properties of these catchments, along with local observation data and the meteorological forcing data of the model, will be described below.

3.1 Experimental data

3.1.1 Rezé catchment

The Rezé experimental site is located in the southern part of the city of Nantes, close to the Atlantic coast (Fig. 2). The experimental site was instrumented (with measurements of precipitation, discharge from the rainwater network and soil water) from 1993 to 1998, and a complete continuous database is available for that period. The climate is oceanic with an average annual rainfall of approx. 830 mm during this period; the year 1994 was the wettest one.

The 4.7-ha basin is entirely residential, comprising single-family homes with private gardens. The separate sewer network is divided into wastewater and stormwater sewers, with lengths of 803 m and 480 m, respectively. The impervious surface of the catchment accounts for 45% of the total area, of which 84% is connected to the stormwater system. A detailed site description can be found in Berthier *et al.* (1999) and Dupont *et al.* (2006) (Tab. 1).

The Rezé catchment and its database have been the subject of several studies (Rodriguez *et al.*, 2003; Berthier *et al.*, 2004; Dupont *et al.*, 2006; Lemonsu *et al.*, 2007; Rodriguez *et al.*, 2008). Berthier (1999) modelled the role of soil in generating urban runoff on the Rezé catchment. He studied both the hydrological aspects and site observations. Among other achievements, he examined the discharge observed in the wastewater sewer during the winter periods between 1993 and 1997, before estimating the discharge due to soil water infiltration, and then compared this value to the simulated base flow in the sewer network.

3.1.2 Pin Sec catchment

The Pin Sec experimental site is located in the eastern section of Nantes; it has been a part of the Nantes Observatory for the Urban Environment (ONEVU) since 2006 and thus contains a dense network of continuous measurement equipment (rain

gauges, flow meters in the sewer networks, piezometers, tensiometers and micro-climatological masts). In correspondence with the simulation period of this study, rainfall patterns were analysed between May 2010 and September 2012, with an annual rainfall of approx. 700 mm recorded for year 2011.

5 The catchment area spans 31 ha and contains some 2,500 inhabitants (Le Delliou *et al.*, 2009). The northern part of the site is characterised by single-family housing with private gardens, as opposed to the southern part, which encompasses 4-storey multi-family buildings with public parks (Fig. 2b). The sewer network is separate, divided into wastewater and stormwater, with respective lengths of 6,973 m and 3,911 m. 51% of the total area is impervious, of which only 61% has been found to be connected to the stormwater sewer (according to a survey conducted by the Nantes Metropolitan government). A description of this catchment is summarised in Tab. 1.

10 **3.2 Meteorological forcing**

Forcing the model with observations requires atmospheric data, such as precipitation, temperature, specific humidity, atmospheric pressure, wind speed and direction, and incoming shortwave and longwave radiation. For both experimental sites, the precipitation rates (no snowfall for all simulation periods) were collected on site by means of rain gauges.

15 All other forcing data were generated from data at the nearby *Météo-France* weather station (at Nantes Airport), including incoming solar radiation, cloudiness, pressure, air temperature and humidity at 2 m above ground, and wind speed at 10 m above ground. To avoid the direct influence of the urban canopy, the forcing level height for temperature, humidity and wind speed had to be set above the roughness sublayer top, hence the atmospheric data had to be adjusted accordingly (Lemonsu *et al.*, 2012b).

4. Evaluation of the TEB-Hydro model

20 The TEB-Hydro model was evaluated by comparing the simulation output with both the observed total stormwater sewer discharge and the portion of this discharge due to soil water infiltration. Observations were derived from the two experimental sites described above. Let's note that the local properties of these sites, as well as the simulation period, do vary. A sensitivity analysis performed on the Rezé catchment will be presented first. The hydrological parameters taken into account consist of: the maximum retention capacity of the artificial surfaces $W_{max,*}^{surf}$ (roads and buildings), a parameter describing the water-tightness of the sewer pipe I_p , the maximum infiltration rate through the road structure I_{rd} , the fraction of impervious surface areas connected to the sewer network f_{con} , and the deep drainage D_* (Sect. 2 and Tab. 2). In addition, possible combined effects of these studied parameters will be analysed. As is typical for hydrological models, this model is calibrated on those parameters where it shows the greatest sensitivity. Next, the model will be evaluated on the observed total stormwater sewer discharge of both the Rezé and Pin Sec catchments. Simulations will be run using the TEB-Hydro model and then compared to observations in order to discuss the performance of recent model developments.

25

30

4.1 Model configuration

The TEB-Hydro model (SURFEX v7.3) has been applied to a single grid point (1D) for both experimental sites; it operates in "off-line" mode, forced by meteorological observations (Sect. 3.2), with a one-hour time step. The model's numerical time step is 5 min. For both catchments, 12 soil layers were taken into account, and the road structure was divided into 5 artificial layers.

5 By virtue of the mean sewer system depth (1.50 m), the sewer pipe is thus situated in the 10th soil layer. Natural surfaces are represented by bare ground, and low and high-growth vegetation.

In the case of the Rezé catchment, the model was run over a 6-year period, from January 1993 to December 1998. The hydrological year starts in September, as the lowest base flow can be detected in August for the Nantes Region. Its morphological data, radiative and thermal properties of materials (TEB), and soil and vegetation properties (ISBA) have all
10 been considered, like in Lemonsu *et al.* (2007).

The simulation period for the Pin Sec catchment is 2.5 years, i.e. between May 2010 and September 2012. The morphological site data, radiative and thermal properties of materials (TEB), and soil and vegetation properties (ISBA) were determined on the basis of several sources (FluxSAP database (Furusho, 2012), Nantes Metropolitan urban databank, and Ecoclimap I (Faroux *et al.*, 2013)). Due to inconsistencies between previous studies (Le Delliou *et al.*, 2009; Seveno *et al.*, 2014), the Pin Sec
15 catchment area has been re-delimited using a GIS (Fig. 2b).

4.2 Sensitivity analysis

The sensitivity analysis was conducted on the Rezé catchment; its aim was to better understand the role of each individual parameter on the various hydrological processes and identify those processes responsible for greater model sensitivity and thus requiring calibration. In general, two types of analyses could be conducted: local and global (Saltelli *et al.*, 2004; Tang *et al.*,
20 2006). For this study, a local analysis based on the One Factor at a Time (OFAT) method was chosen (Montgomery, 2017). This approach measures the influence of a parameter by the amplitude in variation of the model's response around a nominal value of this parameter. The sensitivity analysis encompasses several hydrological parameters, with a range of realistic values (minimum, nominal, maximum). These values have been identified from either a literature review or *in situ* measurements (Hollis and Ovenden, 1988; Berthier *et al.*, 2004; Lemonsu *et al.*, 2007; Ramier *et al.*, 2011; Furusho *et al.*, 2013; Allard,
25 2015) (Tab. 2). The REF simulation is based on the nominal values of all parameters. The MIN and MAX simulations are consistently performed by changing the value of just one parameter with respect to its minimum and maximum values, while all other parameters are fixed at their nominal value.

Moreover, a two-level factorial design of 2^3 is presented in order to determine whether some parameters (I_p , I_{rd} and D_*) display combined effects on the model output and then to dissociate the interactions taking place between them. Such a design is
30 commonly used in experiments involving several interlinked factors (Montgomery, 2007).

Each parameter is assigned two levels, which serves to narrow the experimental domain. In the current case, the domain of each parameter corresponds to the margins set for the sensitivity analysis. Thus, levels +1 and -1 respectively denote the MAX

and MIN values in Tab. 2. To take all possible parameter combinations into account, a matrix is generated with all values being arranged according to the "Yates Order" (Daniel, 1976). The principal effects (Eq. 17) of the given parameters and the effects of their interactions (Eq. 18) are then calculated, in direct correlation with the mean response of both its low level (\bar{y}_{*-}) and high level (\bar{y}_{*+}). The dependence of two parameters can be analysed visually by showing the effects of both parameters on the model response (\bar{y}_*): two perfect parallel lines would not indicate any interdependence between the two factors, as opposed to non-parallelism.

In the current context, \bar{y}_* corresponds to the maximum observed sewer discharge due to soil water infiltration $Q_{\text{sew,max}}$ during winter 1994/95 in the Rezé catchment. A positive effect stands for a gain in of this process while transitioning from the low parameter level (-1) (MIN value) to its high value (+1) (MAX value) and *vice versa* in the case of a negative effect:

$$10 \quad e(A) = \bar{y}_{A+} - \bar{y}_{A-} \quad (17)$$

$$e(AB) = \bar{y}_{AB+} - \bar{y}_{AB-} \quad (18)$$

where $e(A)$ is the principal effect of a parameter called A , $e(AB)$ the effect of the interaction between two different parameters A and B , \bar{y}_{*+} the mean response of all combinations where the parameter or interaction of two parameters is at its high level (+1), and \bar{y}_{*-} the mean response of all combinations where the parameter or interaction of two parameters is at its low level (-1).

4.3 Comparative method

With regards to the sensitivity analysis, the Kling-Gupta statistical criterion (KGE) has been calculated from the output variables of the MIN or MAX simulations as $D_{\text{sim}}(t)$, and from the output variables of the REF simulation as $D_{\text{ref}}(t)$ (Eqs. 19 to 22). For the model calibration and evaluation phase, $D_{\text{ref}}(t)$ is replaced by observed data $D_{\text{obsf}}(t)$. The Kling-Gupta efficiency (KGE) coefficient is a synthesis of several criteria varying between 1 and $-\infty$ (Gupta *et al.*, 2009):

$$KGE = 1 - \sqrt{(r - 1)^2 + (\alpha - 1)^2 + (\beta - 1)^2} \quad (19)$$

with the linear correlation coefficient (r):

$$r = \frac{\sum((D_{\text{sim}}(t) - \overline{D_{\text{sim}}}) * (D_{\text{ref}}(t) - \overline{D_{\text{ref}}}))}{\sqrt{\sum(D_{\text{sim}}(t) - \overline{D_{\text{sim}}})^2} * \sqrt{\sum(D_{\text{ref}}(t) - \overline{D_{\text{ref}}})^2}} \quad (20)$$

with the relative variability (α) represented by the standard deviation:

$$25 \quad \alpha = \frac{\sqrt{\sum(D_{\text{sim}}(t) - \overline{D_{\text{sim}}})^2}}{\sqrt{\sum(D_{\text{ref}}(t) - \overline{D_{\text{ref}}})^2}} \quad (21)$$

and the bias (β):

$$\beta = \frac{\overline{D_{\text{sim}}}}{\overline{D_{\text{ref}}}} \quad (22)$$

The results of the Kling-Gupta efficiency (KGE) criterion are then presented for each MIN and MAX simulation. For this analysis, the chosen model output variables depend on the influence of the parameter on the hydrological processes, namely:

- Total urban runoff (R_{town}) and the subsequent total stormwater sewer discharge (Q_{town}^{tot});
- Sewer runoff due to soil water infiltration into the sewer network (R_{sew}).

5 4.4 Calibration

Based on the outcome of the sensitivity analysis, the TEB-Hydro model is then calibrated. The first few months of the simulation period are systematically excluded, due to the model spin-up in order to allow the model to numerically stabilise. Calibration is applied transversely, meaning that the model is calibrated and evaluated over two different simulation periods. In this manner, the model will first be calibrated over the first period and then evaluated over the second in following the same process, i.e. inverting the calibration and evaluation periods. The simulations are then compared with the observed total stormwater sewer discharge and, like for the sensitivity analysis (Sect. 4.3), the KGE criterion is calculated along with its components.

5. Results and discussion

5.1 Sensitivity analysis

As shown in Tab. 3, the KGE coefficients for the MIN and MAX simulations, specific to the maximum retention capacity of the surface reservoir of roads ($W_{max,rd}^{surf}$) and roofs ($W_{max,rf}^{surf}$), show little difference for both urban runoff and runoff due to soil water infiltration (Figs. 3a and 3b). At maximum roof retention capacity, the urban runoff is mainly influenced by minor rainfall events.

In terms of urban runoff, the model does not show any higher sensitivity to the parameter describing the infiltration rate through the road (I_{rd}) than to $W_{max,rd}^{surf}$ and $W_{max,rf}^{surf}$ (Tab. 3). Such is not the case however when considering sewer runoff due to soil water infiltration (R_{sew}). As the road infiltration rate increases, total urban runoff (R_{town}) decreases but only for minor rain events (Fig. 4a). Also, moisture rises within the soil layers, thus raising soil water infiltration into the sewer network (Fig. 4b). As expected, the model is more sensitive to the fraction of impervious surfaces connected to the stormwater sewer network (f_{con}) (Fig. 5). The bias (β) and relative variability (α) (Tab. 3) reveal different values for MIN and MAX simulations, yet they both lead to the same KGE criterion (Tab. 3). The variation in the f_{con} parameter influences total urban runoff as well as sewer runoff due to soil water infiltration. A low connection rate leads to a lower total urban runoff, while a higher parameter value increases total urban runoff (Fig. 5). The runoff from surfaces not connected to the sewer system feeds infiltration towards the natural surfaces. The amount of infiltrated water in the garden compartment thus changes with this parameter, thereby influencing the soil moisture in all layers and compartments. These values are higher when the fraction of connected surfaces is low and, conversely, lower with a high fraction.

The calculated KGE values (Tab. 3) are quite divergent between the MIN and MAX simulations for parameters I_p and D_* with both output variables, which implies that the model is very sensitive to these parameters. In addition, the results of the factorial design (Fig. 6), based on the calculated direct effects on the maximum sewer discharge due to soil water infiltration, corroborate these results.

5 As regards the parameter describing sewer pipe water-tightness (I_p), its increase leads to higher peaks of infiltration into the sewer network (Fig. 7a) yet does not influence the infiltration period. Moreover, the calculated effect of an I_p of +2.9E-04 signifies an increase in soil water infiltration into the sewer network when transitioning from its low (-1) to high level (+1) (Fig. 6).

As regards the deep drainage parameter (D_*), the negative effect (Fig. 6) indicates that infiltration declines with an increasing parameter value. As observed in Fig. 7b, limiting deep drainage to a magnitude of 10% (MAX) does not generate a significant difference with respect to the reference simulation when assessing sewer discharge due to soil water infiltration. Blocking the deep drainage completely (MIN) however leads to saturation of the lower soil layers, thus adding soil water infiltration into the sewer network (Fig. 7b).

As was the case for sewer pipe water-tightness (I_p), both the infiltration rate through the road (I_{rd}) and deep drainage (D_*) appear to influence sewer drainage due to soil water infiltration, with the effects of their interactions having been calculated and visualised. In this manner, the I_p/D_* interaction can be highlighted as the most influential of all three first-order interactions (Fig. 6). In addition, Figure 8 effectively displays the correlation between the two parameters (see the two lines running non-parallel to one another), whereas correlations between the other parameters appear to be less significant.

In comparing model sensitivity among the 6 parameters for both total urban runoff and runoff due to soil water infiltration, it can be concluded that the model is less sensitive to changes in parameters $W_{\max,rd}^{\text{surf}}$ and $W_{\max,rf}^{\text{surf}}$. Four parameters can thus be singled out for calibration:

- The parameter describing the sewer pipe water-tightness (I_p)
- Infiltration rate through the road (I_{rd})
- The fraction of impervious surfaces connected to the sewer network (f_{con})
- Deep drainage (D_*).

5.2 Model calibration and evaluation

According to the results of the sensitivity analysis, TEB-Hydro needs to be calibrated on four parameters. Yet for both catchment areas, the parameter f_{con} has been determined as a result of exhaustive field surveys and is therefore well known. Consequently, this parameter will be neglected. Hence, only the three remaining parameters are considered for calibration.

30 Four different values within the predefined range of the sensitivity analysis are tested for each parameter (Tab. 4). The model is calibrated and evaluated on the total observed stormwater sewer discharge (Q_{town}^{tot}), as determined from the model outcome variable: total urban runoff (R_{town}). However, since the drainage capacity of soil water through the sewer network can be

extensive in urban areas, the share of sewer discharge originating from soil water infiltration (Q_{sew}) has been investigated in detail. The choice of this parameter value therefore also depends on the findings of the sensitivity analysis with respect to this output variable (Q_{sew}). Section 5.1 showed that soil water infiltration into the sewer increases as the I_p value rises, as opposed to parameters I_{rd} and D_* . The range of values has thus been set close to the maximum I_p value and minimum I_{rd} and D_* values.

5 Totally blocking deep drainage however is not an option, since in reality soil water is not only drained by artificial sewer systems but moreover can find other pathways within the urban subsoil (groundwater recharge, seepage, etc.).

5.2.1 Rezé catchment

As stated above, the calibration step is applied transversely. In the Rezé catchment, the calibration and evaluation periods have been compounded by two consecutive hydrological years, i.e. from September 1993 to August 1995, and from September
10 1995 to August 1997.

The KGE criterion results indicate a clear and constant trend for all simulations, independent of the considered time period (Fig. 9) or the value of parameter D_* , for three reasons:

First, as seen in the example (deep drainage limited to 2%), all KGE criteria are far better for the first period (1993-95) than for the second (1995-97) (Fig. 9). This discrepancy between the two simulation periods is primarily related to the KGE criterion
15 component bias (β), which shows a greater value for the second simulation period (Fig. 9).

Second, the smallest value of I_p achieves a better result than the highest value, when assessing total stormwater sewer discharge (Q_{town}^{tot}). Third, the parameter I_{rd} does not exert any significant influence on the simulated total sewer discharge, since the statistical criterion does not vary significantly among its various values.

The correlation (r) of simulated and observed discharge peaks is satisfactory, with values of approximately 0.90 for both
20 simulation periods and all simulation configurations (Fig. 9). The model displays a tendency to overestimate the observed total sewer discharge (Fig. 10), more so for the second simulation period, in showing greater bias (β) across simulations (Fig. 9).

Regardless of the deep drainage values, simulation 13 seems to stand out. The KGE values range between 0.81 and 0.84 for the first period and between 0.66 and 0.68 for the second. In examining both simulation periods separately, simulation 14 appears to perform slightly better during the first period. Given the fact that simulation 13 performs much better over the
25 second period than simulation 14, simulation 13 should also be tagged for a transversal calibration. The degradation in KGE during the second year is mainly related to the higher bias and variability values, most likely caused by the diverse hydrological properties of both simulation periods. For the first period 1993-95, approx. 1,873 mm of precipitation with a very wet 1994-95 winter can be observed, whereas the second period is much dryer, posting just 1,302 mm. This trend had indeed already
30 been noticed when coupling ISBA with TOPMODEL (Furusho *et al.*, 2013). The soil scheme of ISBA shows slow dynamics in the soil water evolution, thus underestimating the water content under wet weather conditions and overestimating it under dry conditions. The model has been calibrated over the first simulation period under wet weather conditions and evaluated

over a drier period. The soil water and hence total stormwater discharge are raised with parameters D_* and I_p , leading to an overestimation.

As regards total stormwater sewer discharge, the best combination of parameters would consist of setting parameter I_p at 0.09 and I_{rd} at 10^{-5} , whereas parameter D_* is allowed to vary. Depending on the value of parameter D_* , the KGE criterion varies between 0.79 and 0.82 over the entire simulation period. We will thus be examining in greater detail the portion of sewer discharge due to soil water infiltration, with parameter D_* significantly influencing this process. Berthier (1999) observed a maximum sewer discharge due to soil water infiltration of about $0.008 \text{ m}^3 \text{ h}^{-1} \text{ lm}^{-1}$ during winter 1994-95. Accounting for the total sewer length of 1,283 m at the Rezé catchment would yield a maximum sewer infiltration rate of approx. $10.3 \text{ m}^3 \text{ h}^{-1}$. Limiting deep drainage to 2% produces a simulated discharge peak of $4.8 \text{ m}^3 \text{ h}^{-1}$ during this period (Fig. 11a), which is much less than observation findings. In examining the simulation with a limited deep drainage (D_*) of 1%, the observed discharge peak becomes significantly overestimated at $27 \text{ m}^3 \text{ h}^{-1}$ (Fig. 11b). In the aim of evaluating the model as well on the sewer discharge due to soil water infiltration, deep drainage should be limited to somewhere between 1% and 2%.

Another option would consist of focusing on the I_p parameter since the sensitivity analysis also revealed its influence on the process of soil water infiltration into the sewer. As stated above, raising the value of I_p is beneficial for the infiltration rate. Hence, simulation 14 would be more suitable, as I_p has been set at 0.3 while I_{rd} remains at 10^{-5} . In conjunction with deep drainage limited to 2%, the maximum sewer discharge due to soil water infiltration during winter 1994-95 equals approx. $10.6 \text{ m}^3 \text{ h}^{-1}$, which is close to the observed discharge (Fig. 11c). For this combination of parameters (i.e. $I_p=0.3$, $I_{rd}=10^{-5}$, $D_*=2$), the KGE criterion based on total sewer discharge is slightly better, like for simulation 13, with a value of 0.86 for the first period. Such is not the case however for the second period, with a value of 0.57.

5.2.2 Pin Sec catchment

For the Pin Sec catchment, the period between September 2010 and August 2011 has been compared to the period from September 2011 to August 2012 and *vice versa*.

As was the case with the Rezé catchment, the same trends and patterns can be observed independently of the simulation periods and configurations. Simulation 13 is once again cited as the best configuration of parameters, with a KGE criterion of 0.79 over the whole simulation period. Parameter I_p should thus be set at 0.09 and I_{rd} at 10^{-5} , whereas D_* remains variable.

5.2.3 General discussion

In terms of calibration and evaluation processes, TEB-Hydro exhibits the tendency to overestimate the observed total stormwater sewer discharge. This skewing can be explained by the decision to set parameter f_{con} at its documented value rather than calibrating the model on it. This parameter is indeed the one exerting a predominant influence on total stormwater sewer discharge, since it directly influences the surface runoff of impervious surfaces. When calibrating the model on total stormwater sewer discharge, it is thus essential to take this parameter into account should it not be well known, as opposed to

the other parameters I_{rd} and D_* , which exercise little influence over this process. Evaluating the model from the standpoint of sewer discharge due to soil water infiltration however requires a more detailed consideration of I_p and D_* . The water exchanges taking place between the urban subsoil and both the natural and sewer network are critical processes in urban areas. As shown above, the model is very sensitive to them and comparing them to observation findings can help improve the simulated urban water budget, yet experimental data on such fluxes are indeed rare.

For both catchments, the statistical criteria indicate the same trend across all simulation configurations and periods, with a better KGE for the wetter periods. The best simulation configuration is the same irrespective of calibrating the model on the first or second period, with the exception of Simulation 14. It thus proves necessary to apply the model more extensively in regions with different meteorological patterns in order to investigate whether the model could operate under different meteorological conditions (dry and wet periods), which is an essential condition for projection applications. The same simulation configuration yields the best results for both the Rezé and Pin Sec catchments. Considering their differences in terms of soil texture and urban patterns (i.e. mean building height), this result is encouraging for work at the city scale, as spatial heterogeneity no longer constitutes an obstacle.

6. Conclusion

The objective of this study has been to contribute to developing a complete urban hydro-microclimate model and testing the ability of this model to replicate hydrological processes. This goal has been achieved given that the representation of hydrological processes in the TEB-Veg model (Lemonsu *et al.*, 2012a) has been extended and refined. The new model version, called TEB-Hydro, has been developed by taking a detailed representation of the urban subsoil into account. This step has enabled horizontal interactions of soil moisture between the urban subsoil of built-up and natural surfaces within a single grid-cell. Furthermore, soil water drainage via the sewer network has been introduced into the road compartment of the TEB-Hydro model. Deep drainage, which normally supplies the base flow of the natural river network, has been limited to favouring humidification of the lower soil layers. This condition results in more realistic infiltration patterns in the sewer network under urban conditions. A sensitivity analysis has been performed in the aim of better understanding the influences of model parameters on these processes and identifying the parameters to serve for calibration purposes. Six parameters were investigated, with four of them appearing to significantly influence model output in terms of total sewer discharge and the portion of discharge caused by soil water infiltration, namely: parameter (I_p) describing the sewer pipe water-tightness, the road infiltration rate (I_{rd}), the fraction of impervious surfaces connected to the sewer network (f_{con}), and parameter (D_*) that enables limiting deep drainage out of the urban subsoil.

TEB-Hydro was then applied to two small residential catchments located close to the city of Nantes (France). In both cases, the model was calibrated and evaluated on the observed stormwater sewer discharge, in displaying the same hydrological behaviour. Total stormwater sewer discharge is consistently being overestimated, independently of both simulation period and configuration. Considering parameter f_{con} as a calibration element, should it not be known, allows tackling this problem. The

model seems to function better under wet conditions, with superior KGE results. In assessing the entire simulation periods for both catchments, the same parameter configuration stands out, independently of meteorological and local physical conditions, thus implying that the model is running in a coherent and steady manner. This finding would need to be confirmed by applying the model to several catchment areas outside of Nantes. In conclusion, the evaluation outcomes set forth herein are encouraging for model application at the city scale for purposes of projecting global change.

Lastly, a more detailed representation of the urban subsoil and its hydrological pattern enhances the model's urban water budget. Given that water and energy budgets are coupled, it is likely that the energy budget of this model is being influenced at the same time. An upcoming research project now underway entails investigating energy patterns, like latent and sensible heat fluxes, alongside the hydrological processes.

7. Code and data availability

The surface modelling platform SURFEX is accessible on open source, where the codes of surface schemes TEB and ISBA can be downloaded (<http://www.cnrm-game-meteo.fr/surfex/>). This platform is regularly updated; however, the model developments mentioned above have yet to be taken into account in the latest SURFEX (version v8.0). For all further information or access to real-time code modifications, please follow the procedure in order to open the SVN account provided via the previous link. The routines modified with respect to the TEB-Hydro model SURFEX v.7.3, as well as the run directories of the model experiments described above may be retrieved via: <https://doi.org/10.5281/zenodo.1218016>. The Rezé and Pin Sec catchment databases are available upon request submitted to the authors of the Water and Environment Laboratory at the French Institute of Science and Technology for Transport, Development and Networks (IFSTTAR).

Appendix A: List of symbols

20	Q^*	net all-wave radiation (W m^{-2})
	Q_F	anthropogenic heat flux (W m^{-2})
	Q_H	sensible heat flux (W m^{-2})
	Q_E	latent heat flux (W m^{-2})
	ΔQ_S	heat flux storage (W m^{-2})
25	ΔQ_A	net advection heat flux (W m^{-2})
	P	total precipitation ($\text{kg m}^{-2} \text{s}^{-1}$)
	I	water generated from anthropogenic activities (irrigation) ($\text{kg m}^{-2} \text{s}^{-1}$)
	E_*	evapotranspiration over * compartment ($\text{kg m}^{-2} \text{s}^{-1}$)
	R	total runoff ($\text{kg m}^{-2} \text{s}^{-1}$)
30	D_*	deep drainage over * compartment ($\text{kg m}^{-2} \text{s}^{-1}$)

	ΔW	variation in water storage both on the surface and in the ground during the simulation period ($\text{kg m}^{-2} \text{s}^{-1}$)
	L_v	latent heat of vaporisation (J kg^{-1})
	T_*	transfer
	W_*^{surf}	surface retention capacity over * compartment (mm)
5	$W_{max,*}^{surf}$	maximum surface retention capacity over * compartment (mm)
	I_*	surface water infiltration rate of * compartment (m s^{-1})
	R_*^{surf}	surface runoff connected to the sewer network for * compartment (mm s^{-1})
	f_{con}	effective connected impervious area fraction (-)
	R_{sew}	runoff in the sewer network due to soil water infiltration (mm s^{-1})
10	$R_*^{subsurf}$	subsurface runoff from * compartment (mm s^{-1})
	W_*^{gr}	soil moisture content before horizontal balancing over * compartment ($\text{m}^3 \text{m}^{-3}$)
	$W_*^{gr,'}$	soil moisture content after horizontal balancing over * compartment ($\text{m}^3 \text{m}^{-3}$)
	$\overline{W^{gr}}$	mean soil moisture content of all compartments before balancing ($\text{m}^3 \text{m}^{-3}$)
	τ	time constant for one day (s)
15	$\frac{\overline{K_{sat}}}{K_i}$	ratio of the mean hydraulic conductivity at saturation of all three compartments to the hydraulic conductivity of each compartment (-)
	dt	numerical time step of the model (s)
	f_*	surface area fraction of * compartment (-)
	I_p	parameter representing the water tightness of the sewer pipe (-)
20	D_{sew}	sewer density within a single grid cell (-), expressed by the ratio of the total sewer length in one grid cell (m) to the maximum total sewer length in a single grid cell of the entire study site (m)
	$W_*^{gr,n}$	soil moisture content of the last layer n of * compartment ($\text{m}^3 \text{m}^{-3}$)
	$W_*^{gr,flux,n}$	soil moisture content derived from the outgoing water flux of * compartment ($\text{m}^3 \text{m}^{-3}$)
	C_{rech}	coefficient of recharge (-) in order to limit deep drainage
25	d_n	thickness of the last layer
	ρ	water density (kg m^{-3})
	$W_{*,sat}^{gr,i}$	soil moisture content at saturation of * compartment ($\text{m}^3 \text{m}^{-3}$)
	$W_*^{gr,i,'}$	soil moisture content in layer i after update of * compartment ($\text{m}^3 \text{m}^{-3}$)
	$W_*^{gr,i}$	soil moisture content in layer i before update of * compartment ($\text{m}^3 \text{m}^{-3}$)
30	d_i	layer thicknesses of layer i (-)
	$R_*^{subsurf,'}$	subsurface runoff after update of * compartment (mm s^{-1})
	$R_*^{subsurf}$	subsurface runoff before update of * compartment (mm s^{-1})
	$e(A)$	principal effect of a parameter called A (-)
	$e(AB)$	effect of the interaction between two different parameters A and B (-)

	\bar{y}_{*+} (+1) (-)	mean response of all combinations where the parameter or interaction of two parameters is at its high level
	\bar{y}_{*-} (-1) (-)	mean response of all combinations where the parameter or interaction of two parameters is at its low level
5	Q_{town}^{tot}	total stormwater sewer discharge ($\text{m}^3 \text{h}^{-1}$) derived from total urban runoff (R_{town}) ($\text{m}^3 \text{h}^{-1}$)
	Q_{sew}	sewer discharge due to soil water infiltration ($\text{m}^3 \text{h}^{-1}$) derived from sewer runoff (R_{sew}) ($\text{m}^3 \text{h}^{-1}$)
	KGE	Kling Gupta statistical criterion (-)
	r	correlation (-)
	α	variability (-)
10	β	bias (-)
	$D_{sim}(t)$	output variables of MIN and MAX simulations ($\text{kg m}^{-2} \text{s}^{-1}$)
	$D_{ref}(t)$	output variables of the REF simulation. This symbol is replaced by observed data $D_{obsf}(t)$ for purposes of model calibration and the evaluation phase ($\text{kg m}^{-2} \text{s}^{-1}$)
15	with subscripts * standing for:	
	rf	roof
	rd	road
	gdn	garden
	bld	building
20	con	connection
	veg	vegetation
	gr	bare ground surface
	s	sublimation from snow
	sat	saturation
25	sew	sewer
	$rech$	recharge
	max	maximum
	sim	simulation
	ref	reference
30	obs	observation
	v	vertical
	h	horizontal
	with superscripts * standing for:	
35	tot	total
	gr	ground
	$surf$	surface
	$subsurf$	subsurface
	i	layer number
40	n	number of last layer

Competing interests. The authors hereby declare the absence of any conflict of interest.

Acknowledgements. We thank Nantes-Métropole (Direction des Informations Géographiques) for providing the GIS data. We would also like to thank the anonymous reviewers for their helpful comments.

References

- 5 Abramopoulos, F.; Rosenzweig, C. and Choudhury, B.: Improved Ground Hydrology Calculations for Global Climate Models (GCMs): Soil Water Movement and Evapotranspiration, *Journal of Climate*, 1, 921-941, 1988.
- Allard, A.: Contribution à la modélisation hydrologique à l'échelle de la ville: Application sur la ville de Nantes, ED SPIGA, Ecole Centrale de Nantes, Nantes, 2015.
- Bach, P. M., Rauch, W., Mikkelsen, P. S., Mc Carthy, D. T., and Deletic, A.: A critical review of integrated urban water
10 modelling – Urban drainage and beyond . *Environmental Modelling & Software* , 54, 88-107, 2014.
- Belhadj, N.; Joannis, C. and Raimbault, G.: Modelling of rainfall induced infiltration into separate sewerage. *Water Science and Technology* , 32, 161 - 168, 1995.
- Berthier, E.: Contribution à une modélisation hydrologique à base physique en milieu urbain: Elaboration du modèle et première évaluation, Université Joseph-Fourier (UJF), Institut National Polytechnique de Grenoble, Grenoble, 1999.
- 15 Berthier, E., Andrieu, H., and Rodriguez, F.: The Rezé urban catchments database. *Water Resources Research*, 35(6), 1915-1919, 1999.
- Berthier, E., Andrieu, H., and Creutin, J.: The role of soil in the generation of urban runoff: development and evaluation of a 2D model . *Journal of Hydrology* , 299(3–4), 252-266, 2004.
- Berthier, E., Dupont, S., Mestayer, P. and Andrieu, H.: Comparison of two evapotranspiration schemes on a sub-urban site
20 *Journal of Hydrology* , 328, 635 - 646, 2006.
- Betts, R. A.: Implications of land ecosystem-atmosphere interactions for strategies for climate change adaptation and mitigation, *Tellus B. Chemical and Physical Meteorology*, 59:3, 602-615, 2007.
- Boone, A., Masson, V., Meyers, T., and Noilhan, J.: The Influence of the Inclusion of Soil Freezing on Simulations by a Soil–Vegetation–Atmosphere Transfer Scheme. *Journal of Applied Meteorology*, 39, 1544–1569, 2000.
- 25 Bouilloud, L., Martin, E., Habets, F., Boone, A., Moigne, P. L., Livet, J., Marchetti, M., Foidart, A., Franchistéguy, L., Morel, S., Noilhan, J. and Pettré, P. Road Surface Condition Forecasting in France. *Journal of Applied Meteorology and Climatology*, 48, 2513-2527, 2009.
- Daniel, C.: Applications of statistics to industrial experimentation. *John Wiley & Sons*, 124, 1976.
- DHI: Mike Urban cs: Building a simple Mouse Model in Mike Urban. Step-by-step Training Guide, 2001.
- 30 Dupont, S.: Modélisation dynamique et thermodynamique de la canopée urbaine: réalisation du modèle de sols urbains pour SUBMESO, Ecole Doctorale Mécanique Thermique et Génie Civil, Université de Nantes, Nantes, 2001.

- Dupont, S., Mestayer, P. G., Guilloteau, E., Berthier, E. and Andrieu, H.: Parameterization of the Urban Water Budget with the Submesoscale Soil Model. *Journal of Applied Meteorology and Climatology*, 45, 624-648, 2006.
- EC (European Commission): Towards an EU Research and innovation agenda for nature-based solutions and re-naturing cities, Brussels: CEC, 2015.
- 5 EEA: *Urban adaptation to climate change in Europe: Challenges and opportunities for cities together with supportive national and European policies*. Tech. rep., European Environment Agency, EEA Copenhagen, 2012.
- Entekhabi, D. and Eagleson, P. S.: Land Surface Hydrology Parameterization for Atmospheric General Circulation models Including Subgrid Scale Spatial Variability. *Journal of Climate*, 2, 816-831, 1989.
- Faroux, S.; Kaptué Tchuenté, A. T.; Roujean, J.-L.; Masson, V.; Martin, E. and Le Moigne, P.: ECOCLIMAP-II/Europe: a
10 twofold database of ecosystems and surface parameters at 1 km resolution based on satellite information for use in land surface, meteorological and climate models. *Geoscientific Model Development*, 6, 563-582, 2013.
- Fletcher, T., Andrieu, H., and Hamel, P.: Understanding, management and modelling of urban hydrology and its consequences for receiving waters: A state of the art . *Advances in Water Resources* , 51, 261-279, 2013.
- Furusho, C: Base de données FluxSAP IRSTV - Projet ANR-VegDUD, 2012.
- 15 Furusho, C.; Andrieu, H. & Chancibault, K.: Analysis of the hydrological behaviour of an urbanizing basin. *Hydrological Processes*, 28, 1809-1819, 2013.
- Grimmond, C. S. B.; Blackett, M.; Best, M. J.; Baik, J.-J.; Belcher, S. E.; Beringer, J.; Bohnenstengel, S. I.; Calmet, I.; Chen, F.; Coutts, A.; Dandou, A.; Fortuniak, K.; Gouvea, M. L.; Hamdi, R.; Hendry, M.; Kanda, M.; Kawai, T.; Kawamoto, Y.; Kondo, H.; Krayenhoff, E. S.; Lee, S.-H.; Loridan, T.; Martilli, A.; Masson, V.; Miao, S.; Oleson, K.; Ooka, R.; Pigeon, G.;
20 Porson, A.; Ryu, Y.-H.; Salamanca, F.; Steeneveld, G.; Tombrou, M.; Voogt, J. A.; Young, D. T. and Zhang, N.: Initial results from Phase 2 of the international urban energy balance model comparison. *International Journal of Climatology*, John Wiley & Sons, Ltd., 31, 244-272, 2011.
- Gros, A.; Bozonnet, E.; Inard, C. and Musy, M.: Simulation tools to assess microclimate and building energy – A case study on the design of a new district. *Energy and Buildings*, 114, 112 - 122, 2016.
- 25 Gupta, H. V.; Kling, H.; Yilmaz, K. K. and Martinez, G. F.: Decomposition of the mean squared error and NSE performance criteria: Implications for improving hydrological modelling. *Journal of Hydrology*, 377, 80-91, 2009.
- Hamel, P., Daly, E., and Fletcher, T. D.: Source-control stormwater management for mitigating the impacts of urbanisation on baseflow: A review . *Journal of Hydrology* , 485, 201-211, 2013.
- Hollis, G. E. and Ovensen, J. C.: The quantity of stormwater runoff from ten stretches of road, a car park and eight roofs in
30 Hertfordshire, England during 1983, *Hydrological Processes*, 2, 227-243, 1988.
- Le Delliou, A.-L., Rodriguez, F. and Andrieu, H.: Modélisation intégrée des flux d'eau dans la ville - impacts des réseaux d'assainissement sur les écoulements souterrains. *La Houille Blanche*, 152-158, 2009.
- Lemonsu, A., Masson, V., and Berthier, E.: Improvement of the hydrological component of an urban soil–vegetation–atmosphere–transfer model. *Hydrological Processes*, 21(16), 2100-2111, 2007.

- Lemonsu, A., Masson, V., Shashua-Bar, L., Erell, E., and Pearlmutter, D.: Inclusion of vegetation in the Town Energy Balance Model for modeling urban green areas. *Geoscientific Model Development*, 5, 1377-1393, 2012a.
- Lemonsu, A., Kounkou-Arnaud, R., Desplat, J., Salagnac, J.-L., and Masson, V.: Evolution of the Parisian urban climate under a global changing climate, *Climatic Change*, doi:10.1007/s10584-012-0521-6, 2012b.
- 5 Lerner, D. N.: Identifying and quantifying urban recharge: a review. *Hydrogeology Journal*, 10, 143-152, 2002.
- Malys, L.; Musy, M. and Inard, C.: Direct and Indirect Impacts of Vegetation on Building Comfort: A Comparative Study of Lawns, Green Walls and Green Roofs. *Energies*, 9, 2016.
- Mitchell, V. G.; Cleugh, H. A.; Grimmond, C. S. B. and Xu, J.: Linking urban water balance and energy balance models to analyse urban design options. *Hydrological Processes, John Wiley & Sons, Ltd.*, 22, 2891-2900, 2008.
- 10 Masson, V.: A Physically-Based Scheme For The Urban Energy Budget In Atmospheric Models. *Boundary-Layer Meteorology*, 94(3), 357-397, 2000.
- Masson, V.; Le Moigne, P.; Martin, E.; Faroux, S.; Alias, A.; Alkama, R.; Belamari, S.; Barbu, A.; Boone, A.; Bouysse, F.; Brousseau, P.; Brun, E.; Calvet, J.-C.; Carrer, D.; Decharme, B.; Delire, C.; Donier, S.; Essaouini, K.; Gibelin, A.-L.; Giordani, H.; Habets, F.; Jidane, M.; Kerdraon, G.; Kourzeneva, E.; Lafaysse, M.; Lafont, S.; Lebeaupin Brossier, C.; Lemonsu, A.;
- 15 Mahfouf, J.-F.; Marguinaud, P.; Mokhtari, M.; Morin, S.; Pigeon, G.; Salgado, R.; Seity, Y.; Taillefer, F.; Tanguy, G.; Tulet, P.; Vincendon, B.; Vionnet, V. and Voldoire, A.: The SURFEXv7.2 land and ocean surface platform for coupled or offline simulation of earth surface variables and fluxes. *Geoscientific Model Development*, 6, 929-960, 2013.
- Montgomery, D. C.: University, A. S. (Ed.) Design and Analysis of Experiments, John Wiley & Sons Inc., 2017.
- Musy, M.; Malys, L.; Morille, B. and Inard, C.: The use of SOLENE-microclimat model to assess adaptation strategies at the
- 20 district scale. *Urban Climate*, 14, 213 - 223, 2015.
- Oke, T.: *Boundary Layer Climates* (éd. 2d ed). (Routledge, Éd.), 1987.
- Ramier, D.; Berthier, E. and Andrieu, H.: The hydrological behaviour of urban streets: long-term observations and modelling of runoff losses and rainfall–runoff transformation. *Hydrological Processes, John Wiley & Sons, Ltd.*, 25, 2161-2178, 2011.
- Rodriguez, F.; Andrieu, H. and Creutin, J.-D.: Surface runoff in urban catchments: morphological identification of unit
- 25 hydrographs from urban databanks. *Journal of Hydrology*, 283, 146 - 168, 2003.
- Rodriguez, F., Andrieu, H., and Morena, F.: A distributed hydrological model for urbanized areas – Model development and application to case studies. *Journal of Hydrology*, 351(3–4), 268-287, 2008.
- Rossman, L. A.: Storm water management model user's manual, version 5.0 National Risk Management Research Laboratory, Office of Research and Development, US Environmental Protection Agency Cincinnati, 2010.
- 30 Salvadore, E., Bronders, J., and Batelaan, O.: Hydrological modelling of urbanized catchments: A review and future directions. *Journal of Hydrology*, 529, Part 1, 62-81, 2015.
- Saltelli, A.; Tarantola, S.; Campolongo, F. and Ratto, M.: Sensitivity Analysis in Practice: a guide to assessing scientific models, John Wiley & Sons, Ltd, 2004.

Schirmer, M., Leschik, S., and Musolff, A.: Current research in urban hydrogeology – A review . *Advances in Water Resources* , 51, 280-291, 2013.

Seveno, F., Rodriguez, F., de Bondt K. and Joannis C.: Identification and representation of water pathways from production areas to urban catchment outlets: a case study in France, 2nd International Conference on the Design, Construction, Maintenance, Monitoring and Control of Urban Water, Germany, 2014.

Tang, T.; Reed, P.; Wagener, T. and Van Werkhoven, K.: Comparing sensitivity analysis methods to advance lumped watershed model identification and evaluation. *Hydrology and Earth System Sciences Discussions*, 3, 3333-3395, 2006.

Table 1: Summary of basin characteristics for both the Rezé and Pin Sec catchments

Description		Rezé	Pin Sec
Surface area		4.7 ha	31.3 ha
Housing type		Residential (individual)	Residential (individual and multi)
Mean building height (H_{mean})		5.9 m	9.3 m
Land use	garden	55%	49%
	building	17%	19%
	road	28%	32%
Soil texture	clay	40%	8%
	sand	38%	51%
Imperviousness of the surface area		45%	51%
Impervious surfaces connected to the sewer		84%	61%
Length of sewer network	wastewater	803 m	3,911 m
	storm drain	480 m	6,972 m
Mean sewer depth		1.50 m	1.50 m

5

10

15

Table 2: Description of the hydrological parameters of the TEB-Hydro model as well as its MIN, MAX and REF values for the sensitivity analysis. The deep drainage values correspond to a coefficient of recharge of respectively 1.0, 0.95 and 0.90. The values for $W_{max,rd}^{surf}$, $W_{max,rf}^{surf}$, I_{rd} et f_{con} have been identified from either a literature review or *in situ* measurements ([^]Hollis and Ovenden (1988); ^{*}Berthier *et al.*, 2004; ⁺Lemonsu *et al.*, 2007; [#]Ramier *et al.*, 2011; [°]Furusho *et al.*, 2013; [·]Allard, 2015)

Simulation	Parameter	Description	Unit	Values		
				MIN	REF	MAX
SROAD	$W_{max,rd}^{surf}$	Maximum retention capacity of the road surface reservoir	mm	0.5 ^{(+),(°)}	3.0 ^(*)	6.0 ⁽⁺⁾
SROOF	$W_{max,rf}^{surf}$	Maximum retention capacity of the roof surface reservoir	mm	0.25 ^{(^),(*)}	1.5 ^(°)	3.0 ^(°)
IP	I_p	Parameter describing the sewer pipe water-tightness	-	10 ⁻³	10 ⁻¹	1
IROAD	I_{rd}	Infiltration rate through the road	m s ⁻¹	10 ⁻⁹ ^{(+),(°),(#),(*)}	10 ⁻⁶	10 ⁻⁵ ⁽⁺⁾
CONN	f_{con}	Effective fraction of impervious surfaces connected to the sewer network	-	0.5 ⁽⁻⁾	0.7 ⁽⁻⁾	0.9 ^{(°),(-)}
DRAIN	D_*	Deep drainage	%	0	5	10

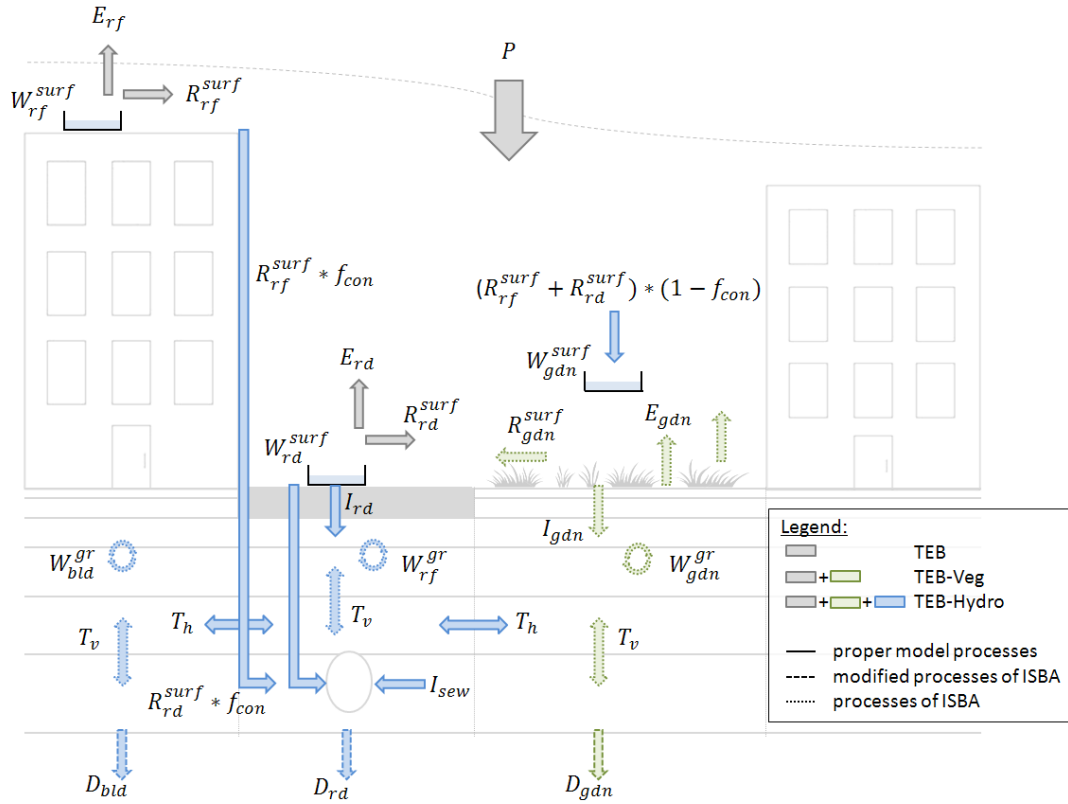
5

Table 3: Statistical criteria (r, α , β , KGE) based on the model output variables, as calculated between the MIN and MAX simulations, for each parameter and the reference simulation (REF)

Output variable	Simulation	Parameter	MIN criteria				MAX criteria			
			r	α	β	KGE	r	α	β	KGE
Q_{town}^{tot}	SROOF	$W_{max,rf}^{surf}$	1.00	1.01	1.06	0.94	1.00	0.99	0.96	0.96
	SROAD	$W_{max,rd}^{surf}$	0.99	1.04	1.11	0.88	0.99	0.96	0.94	0.93
	IROAD	I_{rd}	1.00	1.00	1.01	0.99	1.00	0.98	0.94	0.94
	CONN	f_{con}	1.00	0.73	0.75	0.64	1.00	1.28	1.25	0.63
	IP	I_p	1.00	1.00	0.93	0.93	1.00	1.01	1.41	0.59
	DRAIN	D_*	0.91	1.20	1.80	0.17	1.00	1.00	0.99	0.99
Q_{sew}	SROOF	$W_{max,rf}^{surf}$	1.00	1.01	1.06	0.94	1.00	0.99	0.96	0.96
	SROAD	$W_{max,rd}^{surf}$	0.99	1.04	1.11	0.88	0.99	0.96	0.94	0.93
	IROAD	I_{rd}	1.00	0.99	0.99	0.98	1.00	1.05	1.09	0.90
	CONN	f_{con}	0.99	1.19	1.21	0.72	0.98	0.82	0.78	0.72
	IP	I_p	1.00	0.01	0.01	-0.40	0.99	7.43	7.0	-7.79
	DRAIN	D_*	0.78	20.51	11.47	-21.14	1.00	0.90	0.84	0.81

Table 4: Range of values on each parameter tested for use in calibration

$I_p[-]$	0.09	0.3	0.6	1
$I_{rd}[\text{mm s}^{-1}]$	10^{-8}	10^{-7}	10^{-6}	10^{-5}
$D_*[\%]$	1	2	3.5	5



5 **Figure 1: Diagram of the hydrological processes involved in the TEB-Hydro model; subscripts *rf* and *bid* stand for building compartment, *rd* for road compartment, and *gdn* for garden compartment**

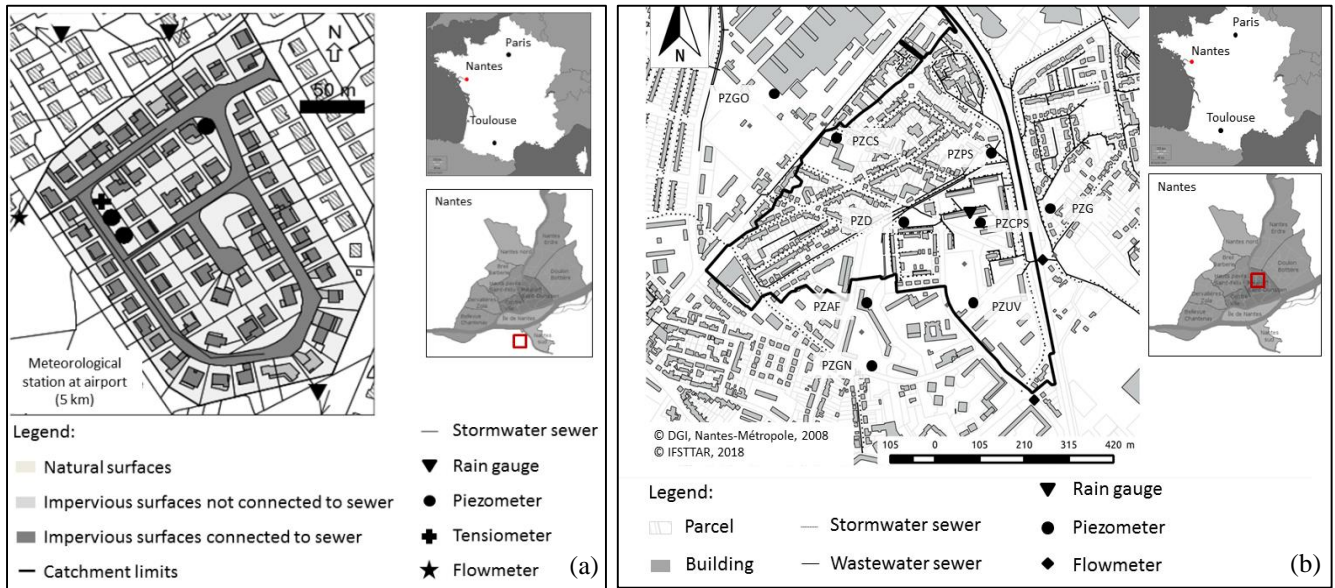
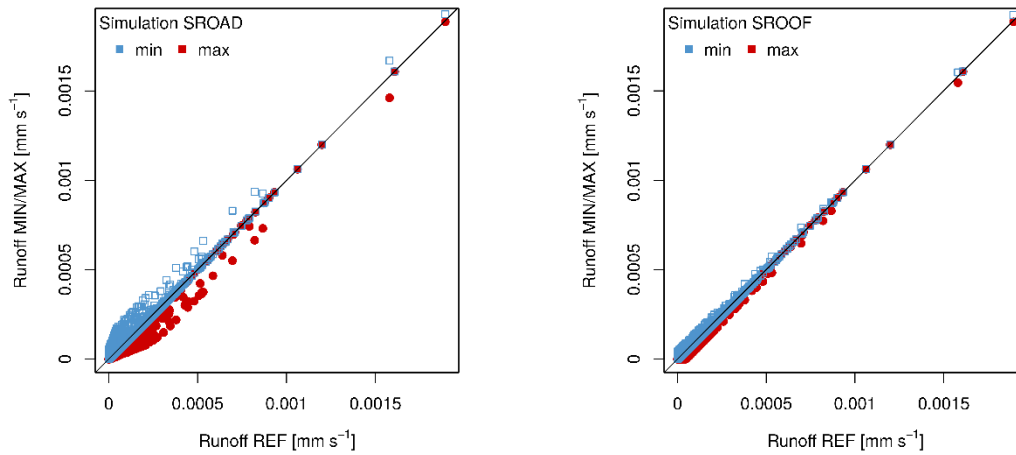


Figure 2: a) the Rezé experimental site (from Dupont, 2001); b) the Pin Sec experimental site. Maps to the right of the catchments indicate the location of Nantes (France) above and the Rezé and Pin Sec catchment locations (red square) in Nantes (middle)



5 Figure 3: Comparison of urban total runoff (R_{town}) between the reference simulation (REF) and both the MIN simulation (shown in blue) and MAX simulation (red) for the parameters: a) $W_{max,rd}^{surf}$ (left side), and b) $W_{max,rf}^{surf}$ (right side).

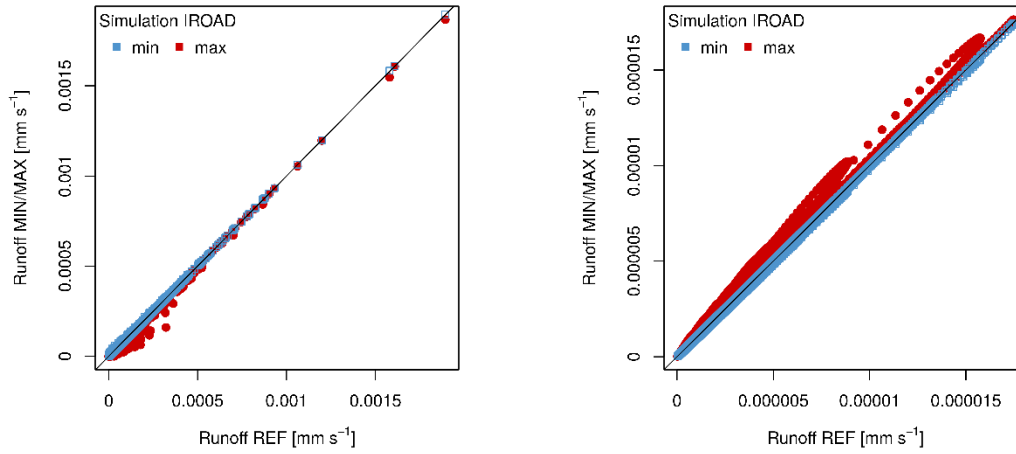
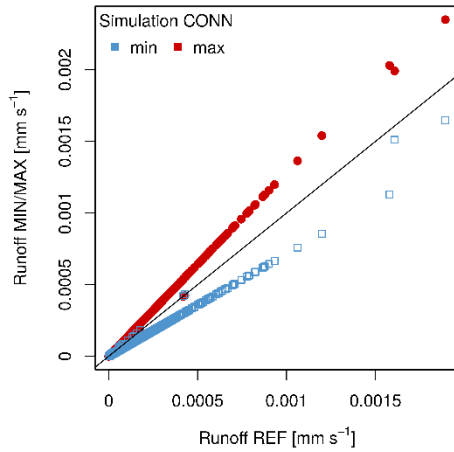


Figure 4: a) Comparison of urban total runoff (R_{town}) between the reference simulation (REF) and both the MIN simulation (blue) and MAX simulation (red) for parameter I_{rd} on the left side; and b) comparison of the sewer runoff due to soil water infiltration (R_{sew}) between the reference simulation (REF) and the MIN (blue) and MAX (red) simulations for parameter I_{rd} on the right side



5

Figure 5: Comparison of total urban runoff (R_{town}) between the reference simulation (REF) and the MIN (blue) and MAX (red) simulations for parameter f_{con}

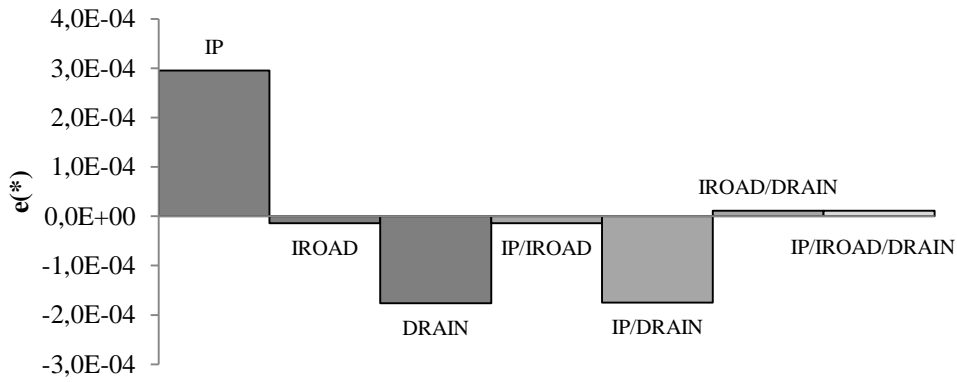
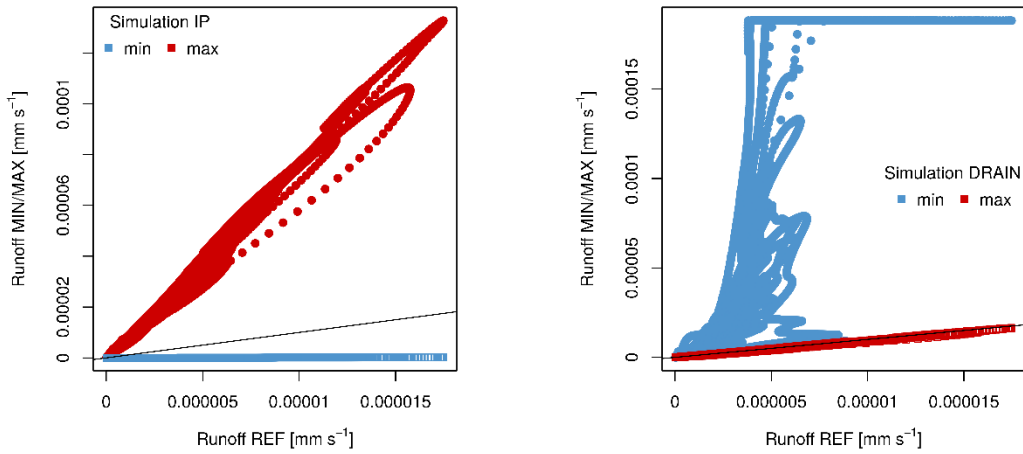


Figure 6: Calculated effects on the model response (R_{sew}) from parameters I_p , I_{rd} and D_* and their interactions. (dark shade of grey: principal effects, middle grey: second-order effects, and light grey: third-order effects)



5 **Figure 7:** Comparison of sewer runoff due to soil water infiltration (R_{sew}) between the reference simulation (REF) and the MIN (blue) and MAX (red) simulations for parameters a) I_p (left side), and b) D_* (right side)

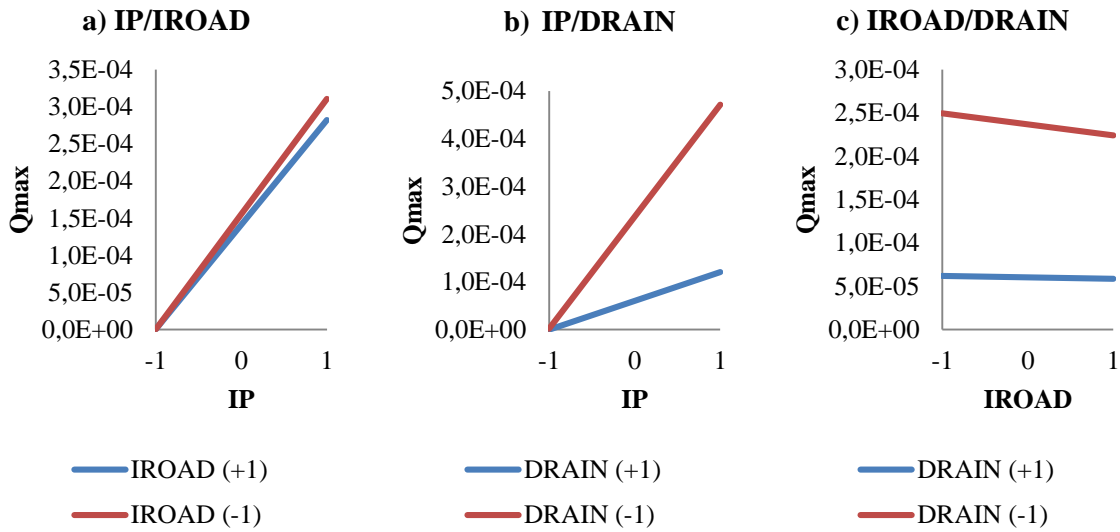
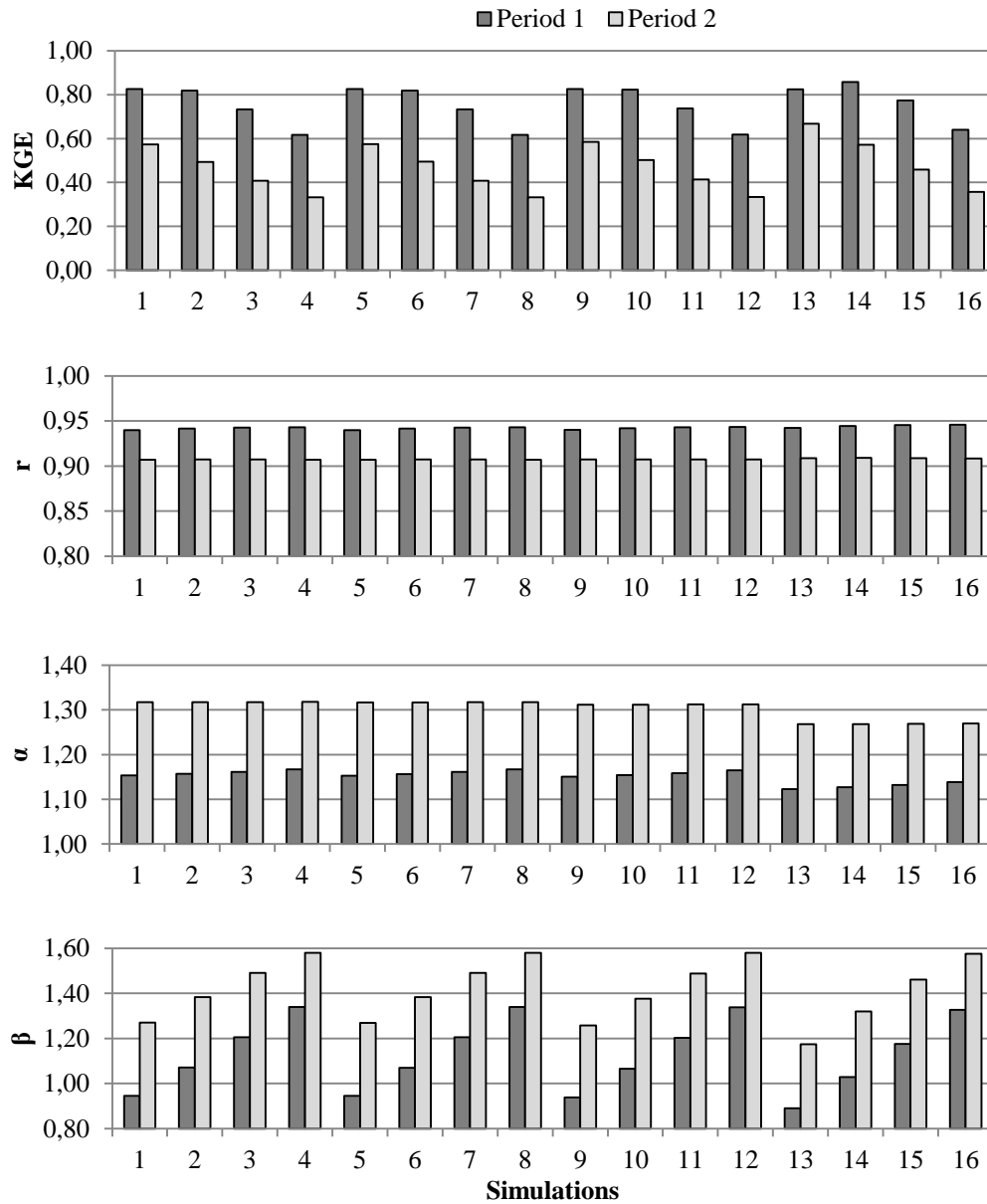


Figure 8: Interactions as a function of the maximum observed sewer runoff due to soil water infiltration during the 1994-95 winter of the second order between parameters: a) I_p and I_{rd} ; b) I_p and D_* and of the third order between parameters: c) I_p , I_{rd} , and D_*



Simulations	1	2	3	4	5	6	7	8	9	10	11	12	13	14	15	16
I_p	0.09	0.3	0.6	1	0.09	0.3	0.6	1	0.09	0.3	0.6	1	0.09	0.3	0.6	1
I_{rd}	10^{-8}	10^{-8}	10^{-8}	10^{-8}	10^{-7}	10^{-7}	10^{-7}	10^{-7}	10^{-6}	10^{-6}	10^{-6}	10^{-6}	10^{-5}	10^{-5}	10^{-5}	10^{-5}
D_*	2	2	2	2	2	2	2	2	2	2	2	2	2	2	2	2

5 Figure 9: Example of a calculated criterion for the simulation configurations where parameter D_* (deep drainage) is limited to 2% and all other parameters allowed to vary. The KGE criterion, the correlation criterion (r), the variability criterion (α) and the bias (β) for all 16 simulations and for the first (dark grey) and second (light grey) simulation periods are shown.

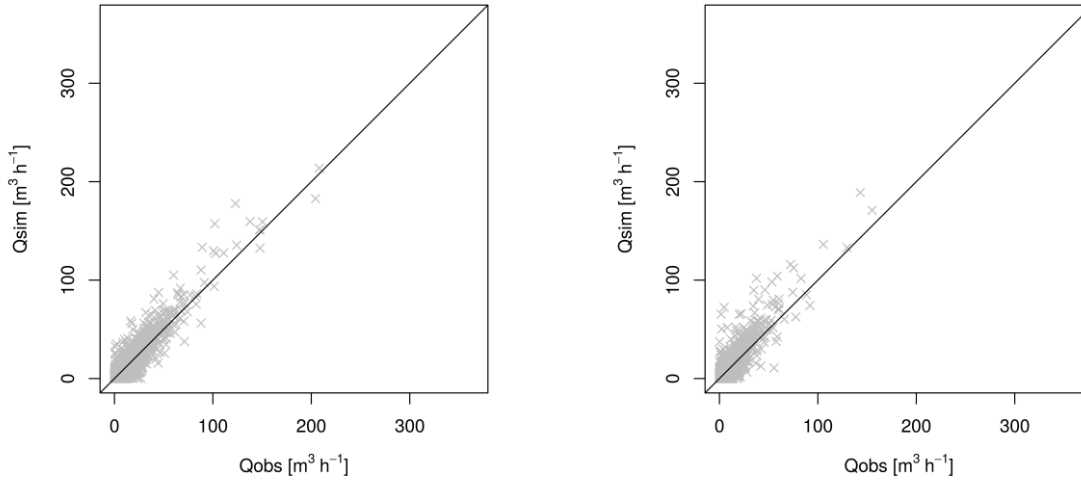
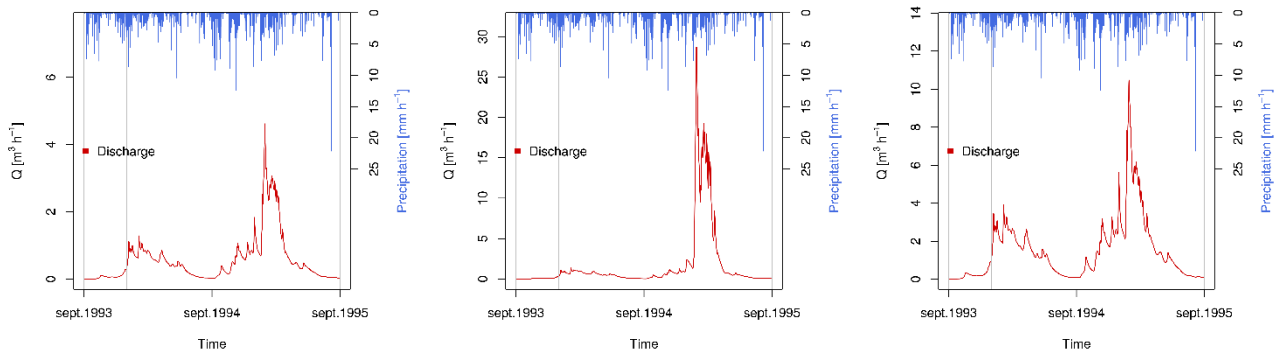


Figure 10: Comparison of simulated and observed total stormwater sewer discharge [$\text{m}^3 \text{h}^{-1}$] during: a) the first simulation period from September 1993 to August 1995 (left side); and b) the second simulation period from September 1995 to August 1997 (right side) for Simulation 13 and a deep drainage limited to 2%



5

Figure 11: Simulated sewer discharge due to soil water infiltration [$\text{m}^3 \text{h}^{-1}$] during the first simulation period 1993-95 based on the combination of parameters I_p set at 0.09 and I_{rd} set at 10^{-5} and: a) D_* limited to 2%, b) D_* limited to 1%, and c) based on the combination of parameters I_p set at 0.3, and I_{rd} set at 10^{-5} , with a D_* value limited to 2%